Journal of Network Intelligence
Taiwan Ubiquitous Information
 ISSN 2414-8105
Volume **9**, Number **4**, November **2024**

Hydroelectric Generator Excitation Control Based on Improved Genetic and RBF Neural Networks

Hao-Zhi Liu*

Division of Continuing Education
Nanchong Vocational and Technical College, Nanchong 637100, P. R. China
Haozhi2212@126.com

Yuan Li, Zhong-Guo You, Jian-Qiang Ming

Department of Mechanical and Electrical Engineering
Nanchong Vocational and Technical College, Nanchong 637100, P. R. China
liyuanzengyan@163.com, nczy321@163.com, ncming2023@126.com

Andrew Liu

College of Information Science
Mapúa University, Intramuros, 1002 Metro Manila, Philippines
pm8659@163.com

*Corresponding author: Hao-Zhi Liu
Received December 17, 2023, revised March 7, 2024, accepted June 6, 2024.

Abstract. *Aiming at the feature of hydro generator excitation control system such as large inertia, large hysteresis and unstable parameters, a hydro generator excitation control on the ground of enhanced Genetic Algorithm (GA) and Radial Basis Function (RBF) neural network is designed. Firstly, for the issue of convergence of GA, the computational framework of GA is improved relied on the coarse-grained parallel computing model, and at the same time, for the defects of GA, the adaptive strategy is adopted to optimize the design of the main steps of the objective function, crossover, variation and migration of the population evolution. Then, on the ground of the enhanced GA, the RBF neural network learning model is selected, the neural network weights are coarsely and finely tuned by gradient descent method and GA, respectively, and the internal and external perturbations of the system are estimated by the expanding state discover, and the nonlinear state-error feedback manage law is combined with the excitation engine manage strategy for the purpose of dealing with the issues of system inertia, hysteresis and perturbation. The simulation outcome indicates that in the excitation starting process, load step and load dumping, the overshoots of the hydro generator excitation manage system designed relied on the enhanced GA and RBF neural network in this paper are 16.94%, 7.14% and 23.83%, respectively, which are 2.57%, 2.47% and 2.91% lower than those of the excitation control algorithm with the imposed disturbance observer, and the system's anti-disturbance capability and robustness are effectively enhanced.*
Keywords: Hydroelectric generator; Excitation control; Genetic algorithm; RBF neural network; Adaptive strategy

1. **Introduction.** With the increasing scale and complexity of the hydraulic system, the requirements for the energy transmitting level of the hydraulic system are becoming higher and higher, once the stability of the system operation is destroyed, it will lead to the national economy to suffer a significant loss, and bring a significant impact on people's lives. Therefore, improving the security and constancy of system operation has

become an increasingly important and urgent research topic [1, 2, 3]. The inflammation system is the core of synchronal generator operation control has a direct impact on the reliability, economy and other characteristics of generator operation. The inflammation system is to adjust the inflammation voltage at both sides of the hydraulic generator, so as to regulate the electric potential of the engine and achieve the purpose of stabilizing the depot voltage. Aiming at guaranteeing the normal operation of the synchronous generator, the inflammation system could stably offer the inflammation recent needed by the synchronous generator from no-load to full-load and overload [4, 5]. During the accident function procedure, the synchronous generator inflammation control system also takes a very significant part: when the power system faults and the grid voltage drops, the inflammation system could quickly force inflammation, to enhance the stability of the system. When the synchronous generator short-circuit faults occur within the synchronous generator, in order to rapidly eliminate the fault and make the fault confined to the smallest possible range, it should be able to quickly extinguish the magnetization.

1.1. **Related Work.** The growth of hydroelectric generator excitation control theory has gone through the process from single-variable to multi-variable, from linear to nonlinear, and finally to the direction of intelligent control. Xia and Heydt [6] proposed a single-output-single-input excitation control method with proportional regulation according to generator-side voltage deviation. However, Devotta [7] proposed Proportional Integral Derivative (PID) restrain by generator-side voltage digression. Schaefer and Kim [8] proposed that PID regulation improves the sluggish and temporary stability of the system to a certain extent, but still fails to effectively solve the contradiction between the regulation accuracy and stability. Galaz et al. [9] pointed out that both proportional voltage regulation and PID regulation do not have a good control effect, and PID regulation cannot actually enhance the active quality of the system and increase the stability level of the system. Aiming at enhancing the contradiction between the precision and stability of the PID excitation method and the lack of artificial damping, Malik [10] proposed the auxiliary excitation control strategy using power system stabilizer based on the phase compensation principle to form an excitation controller with the structure of "AVR + PSS". Maya-Ortiz and Espinosa-Pérez [11] proposed a combination of robust and adaptive design method, PSS from the initial single-variable design to the dual-variable feedback PSS. Fan et al. [12] developed a strongly excited excitation regulator, the introduction of auxiliary feedback, the use of the "D-domain division method" to determine the parameters of the common stabilization domain. Univariable based control methods usually only consider the relationship between a single input and a single output, and ignore other factors that may affect the excitation control. The multi-variable based control method can consider the complex interaction of multiple inputs and outputs, so as to achieve more precise control, but it also increases the complexity and calculation amount of the control system.

As modern control theory and control practice developing, the research methods and tools have been enhanced continuously. Fusco and Russo [13] proposed to apply the optimal control theory to the hydraulic system. Saavedra-Montes et al. [14] firstly established and perfected the theoretical system of linear optimal excitation controllers, which lacks the sufficiently high voltage feedback and gain in comparison to the AVR/PSS-type excitation controllers. Zhao et al. [15] started to apply the adaptive control theory to the design of excitation controllers, the goal of which is to modify the controller parameters or adjust the control strategy to achieve the best control effect. Roy et al. [16] relied on the reference module of the adaptive excitation control system. Wang et al. [17] suggested a way for the design of a nonlinear feedback decoupling controller for generator excitation

in multi-machine power systems by using differential geometric control theory. feedback decoupling controller design method. Nan et al. [18] proposed a nonlinear Terminal sliding mode variable structure excitation controller on the classical sliding mode control, and achieved better excitation results. Baesmat and Bodson [19] proposed the cloud model approach, which is to introduce probabilistic statistical ideas on the traditional fuzzy set theory, constituting a mutual mapping relationship between qualitative and quantitative. Orchi et al. [20] proposed a nonlinear zero dynamic approach to achieve constant reactive power and constant power factor control of small units. Kawabe et al. [21] proposed the use of mamdani-type fuzzy control and fuzzy control in combination with PID for excitation control, which is more effective. Erol [22] combined genetic algorithms and sensitivity-based parsing approach, to Using PMU online data to identify the dominant parameters of the excitation controller. Jankee et al. [23] introduced a synchronous generator inverse structure from the generator third-order model equations, combined with a BP neural network to control the excitation of the generator, and the simulation effect is better. Agarala et al. [24] proposed a doubly-fed excitation control scheme based on a single neuron adaptive PID algorithm, which could the excitation of the doubly-fed generator is adjusted according to the change of wind speed.

1.2. **Contribution.** The various excitation control methods mentioned earlier have their own advantages and shortcomings, and each control strategy has good results in solving a certain aspect of the problem, but often there are hard to deal with issues in the design or control process. Therefore, this article suggests a hydroelectric generator excitation control on the ground of enhanced Genetic Algorithm (GA) and Radial Basis Function (RBF) neural networks. Firstly, the GA is optimized, with the help of parallel evolution of multiple populations, which can accelerate the search of variable space and can increase the overall size of the population, as well as the evolutionary isolation of each subpopulation from each other, which can help to maintain the diversity of the population, avoid falling into the locally optimum solution and improve the quality of the solution. Then a hydro generator excitation control method on the ground of enhanced GA and RBF neural network is designed, and the whole structure of RBF network is divided into stimulus layer, defuzzification layer, fuzzy illation layer and output layer. To avoid using too large a range of excitation control parameters, the slope declivity method is adopted to correct the initial parameters, and then the improved GA is adopted to search for the optimization around this group of parameters to enhance the whole performance of excitation control. At last, the whole performance of the excitation control is enhanced by analyzing the output stabilization value. Finally, this paper verifies the excitation control effect through the output stabilization value, overshooting amount, regulation time and vibration times. The outcome indicates that the excitation control mechanism suggested can ensure the system stability and meet the load demand, thus verifying the effectivity and feasibility of the suggested method and control strategy.

2. Theoretical Analysis.

2.1. **RBF Neural Network.** An RBF neural network is a two-level feedforward network which contains one obscured level [25], [26], the structure of which is shown in Figure 1. It adopts a radial reliable function to match the input directly to the obscured level, and then the output level is obtained through weighting the obscured level, which broadly behaves non-linearly. A Gaussian operation is used as the radial basis function since it is radially proportionate and has random order derivatives. The l-th obscured neuron's response to the stimulant vector $x_j (j = 1, 2, ..., M)$ is:

$$\psi_l(x_j) = \exp\left(-\frac{\|x_j - d_l\|^2}{2\theta_l^2}\right) \tag{1}$$

where $\|\cdot\|$ is the Euclidean paradigm, d_l is the focus vector, and θ_l is the broadness of the l-th obscured neuron, attentively, and $l = 1, 2, ..., L$. The effective output of the Gaussian function is distributed within a narrow window, beyond which it is close to 0. The harvest of the network is produced by an easy linear function, and the output of the Gaussian operation is in Equation (2):

$$y_j = f(x_j) = \sum_{l=1}^{L} h_l \psi_l(x_j) \tag{2}$$

where h_l is the weight that connects the l-th obscured neuron to the harvest neuron.

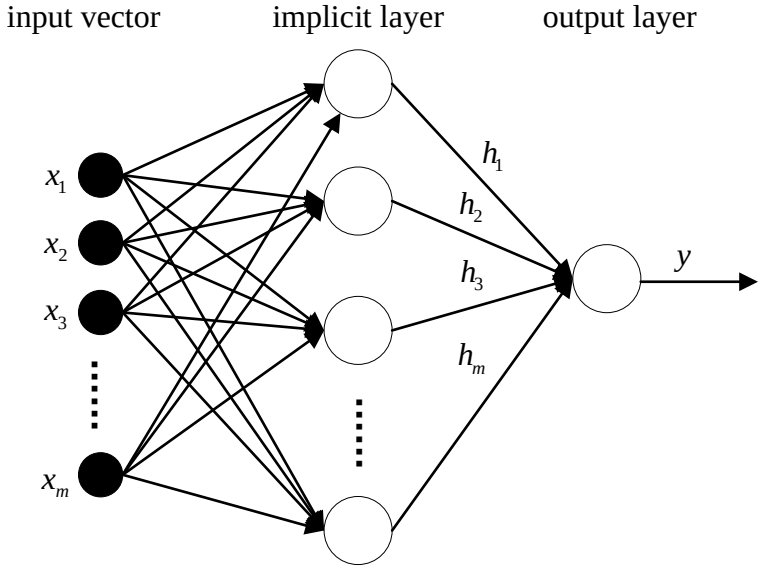

Figure 1. RBF neural network structure

The studying progress of RBF neural network makes up of two phases. The original stage is to clump every instance on the ground of the Euclidean distance among the stimulus and the center; the second stage is to achieve h_l of the clustered samples based on the Recursive Least Squares (RLS) method. The RBF artificial neural network starts without neurons and adds novel neurons through the discipline progress.

(1) Suppose there are already q obscured neurons. Find the stimulus vector with the largest Euclidean range c_{max} through focus vector $d_l (l = 1, 2, ..., Q)$. The farthest range is denoted as follows.

$$c_{max} = \max \|x_j - d_l\| = \|x_s - d_t\| \tag{3}$$

where x_s and d_t are the farthest stimulus vector and focus vector, individually.

(2) Add an obscured neuron with a focus vector equivalent to x_s.

$$\begin{cases} c_{q+1} = x_s \\ \theta_{q+1} = \frac{1}{2}\left(\sum_{i=1}^{2} \|x_s - d_i\|^2\right)^{1/2} \end{cases} \tag{4}$$

where d_i are the two abutting focus vectors of the novel neuron, $i = 1, 2$.

(3) The weights among the obscured level and the instance output level y_j are recreated by the RLS.

(4) The output y_j of the network to x_j is computed through Equation (3) and Equation (4) to obtain the mean square error e as:

$$e = \frac{1}{M}\left(\sum_{l=1}^{m} \|y_j - y_l\|^2\right)^{1/2} \tag{5}$$

If e is less than θ, cultivating is complete; otherwise, give back to Step (1).

Compared with other control algorithms, RBF neural networks are famous for their nonlinear approximation ability. In the excitation control of hydrogenerator, the system may involve complex nonlinear relations. RBF neural network can better fit these nonlinear functions and provide more accurate modeling and control.

2.2. **Hydro generator excitation system.** The inflammation control system is one of the main control links of the hydroelectric generator [27], which regulates the size of the generator induced electromotive force by controlling the output of the excitation power link, and stabilizes the generator output voltage when the load of the power system changes. The hydro generator excitation controller model is indicated in Figure 2.

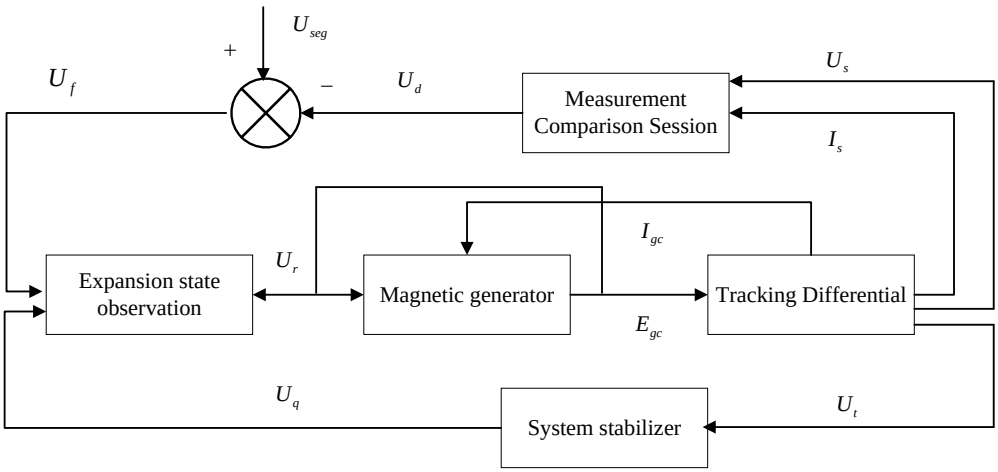

Figure 2. The hydro generator excitation controller model

The meanings of the parameters in the figure are as follows: U_s is the generator terminal voltage; I_s is the generator stator current; U_d is the measurement and comparison link output voltage; E_{gc} is the exciter output voltage; U_t is the integrated amplification control link output voltage; U_r is the voltage feedback control quantity; U_q is the voltage feedback link output quantity; I_{gc} is the generator excitation current; U_{seg} is the reference voltage of the exciter; U_f is the excitation controller voltage deviation.

In the modeling process of the generator link, the first order inertial link is used to represent the mathematical model of the generator.

$$V_v = \frac{L_v}{1 + S_v T} \tag{6}$$

The voltage measurement and comparison unit of the generator is divided into two parts: measurement and comparison. Measurement link from the transformer to measure the generator stator induced electromotive force, and then through the rectifier and filtering link, the stator induced electromotive force will be converted into DC RMS value

according to the proportionality relationship. Then, the DC RMS value will be input to the comparison link, and then the divergence between the true value of the stator electromotive force and the rated value will be computed, and the difference will be taken as the final output of the unit. The association between the output U_d of the unit and the stator induced electromotive force is shown in Equation (7).

$$U_d = |\dot{U} + (L_d + ix_d)| \tag{7}$$

Expansion of the state observation unit through the input signal voltage deviation signal amplification, and limiting control and other operations, to provide the synchronous trigger unit with the required control signals, through the silicon controlled rectifier regulating the output of the system, as shown in Equation (8).

$$G_A(T) = \frac{L_B}{1 + S_B T} \cdot \frac{L_L}{1 + S_L T} \cdot \frac{L_C}{1 + S_C T} = \frac{L_A}{1 + L_A T} \tag{8}$$

where $L_A = L_B L_L L_C$ is the scaling factor for the expansion state observation link, and the time response factor $S_A = S_C$.

3. **Improved Genetic Algorithm.** Utilizing the natural parallelizability of GA, the initial population is separated into multiple sub-populations, each sub-population performs genetic operations concurrently without interfering with each other, and after a certain number of generations the individuals of the sub-populations perform migration operations, which not only promotes the transmission of good individuals among different sub-populations, but also enriches the variety of the population and reduces the phenomenon of immature-as-corner [28]. The parallel genetic algorithm based on this concept is suitable for solving complex multidimensional problems, and with the help of parallel evolution of multiple populations, it can accelerate the search of variable space, and can increase the overall size of the population, as well as evolutionary isolation of sub-populations from each other, which helps to maintain the diversity of the population, avoid falling into the native ideal solution, and improve the quality of the solution.

In this paper, the computational framework of GA is improved based on the coarse-grained parallel computing model, and at the same time, for the defects of GA algorithm, an adaptive strategy is adopted to optimize the design of the main steps of the objective function, crossover, mutation, and migration of the population evolution. The flow of the improved GA is shown in Figure 3. The coarse-grained parallel computing model is a kind of parallel computing model, which is characterized by decomposing the whole computing task into relatively large blocks or task units, and then processing these larger units in parallel.

(1) Optimization of objective function. In order to better control the total amount of water consumption, peak flow rate, and peak time, combined with the hydrological intelligence forecast specification, this paper takes the total amount of water consumption qualification rate PS_g, the peak flow qualification rate PS_q, and the peak time qualification rate PS_t as the objective operation.

$$F = \max(f_1 * PS_g + f_2 * PS_q + f_3 * PS_t) \tag{9}$$

where F is the objective function and is a positive indicator, which can be directly used as the fitness function. $f : f_1, f_2, f_3$ are the weights of the three objective functions.

(2) Crossover mutation. In order to avoid premature maturity of GA and enhance the native seek ability and convergence of the algorithm, the adaptive strategy can make the values of crossover and mutation processes more reasonable and effective. When the population evolves to a certain stage, some individuals in the population gradually converge to the optimal solution, a large number of identical individuals appear, and the

population dispersion decreases. Thus, the population dispersion can be used to react to the degree of evolution of the population. This paper designs the population dispersion coefficient η with Equation (10).

$$\eta_s = \frac{\sum_{j=1}^{q} \sum_{i=1}^{l} \left(\frac{x_{ij} - l_j}{l_j}\right)^2}{q} \tag{10}$$

where s is the number of iterations of the current population, x_{ij} is the value of the j-th variable for the i-th individual in the population, q is the population size, h is the number of variables, and l_i is the mean value of the variable.

For the problem of early maturity of the population, combined with the population discrete coefficients, this paper designed the adaptive genetic algorithm crossover probability P_d and variance probability P_n.

$$P_d = l_1 + l_2 \frac{f_{\max} - f'}{f_{\max} - f_{\min}} \frac{\eta_s}{t_0} \tag{11}$$

$$P_n = l_3 + l_4 \frac{f_{\max} - f}{f_{\max} - f_{\min}} \frac{\eta_s}{t_0} \tag{12}$$

where $l_1 - l_4$ are the adaptive control parameters, f' is the larger of the fitness values of the two individuals in the crossover operation, $f_{\min}$ and $f_{\max}$ are the smallest and largest values of the fitness function, respectively, and η_s/t_0 is the decrement function, which gradually converges to 0 as the population evolves.

The Simulated Binary Crossover (SBX) method is used as the crossover operator and is calculated as follows:

$$d_1 = 0.5\left((1+\alpha)p_1 + (1-\alpha)p_2\right) \tag{13}$$

$$d_2 = 0.5\left((1-\alpha)p_1 + (1+\alpha)p_2\right) \tag{14}$$

where p_1 and p_2 are the parents before crossover, and d_1 and d_2 are the offspring generated by crossover. α is the distribution factor.

The Polynomial Mutation (PM) method is used as the mutation operator, which mainly enhances the native search capability of GA and prevents premature convergence. It is calculated as follows:

$$g_i' = g_i + \theta(w_i - k_i) \tag{15}$$

$$\theta = \begin{cases} \left[2u_n + (1-2u_n)(1-\theta_1)^{(\mu_n+1)}\right]^{1/(\mu_n+1)} - 1, & u_n \le 0.5 \\ 1 - \left[2(1-u_n) + (2u_n-1)(1-\theta_2)^{(\mu_n+1)}\right]^{1/(\mu_n+1)}, & u_n > 0.5 \end{cases} \tag{16}$$

$$\theta_1 = \frac{(g_i - k_i)}{(g_i - k_i)} \tag{17}$$

$$\theta_2 = \frac{(w_i - g_i)}{(w_i - k_i)} \tag{18}$$

where g_i is the parent before mutation, g_i' is the offspring generated by mutation, w_i is the upper limit of the variance, k_i is the lower limit of the variance, θ is the coefficient of variation, u_n is a random number in the interval [0, 1], and μ_n is the distribution index of the variance.

(3) Migration. Based on the discrete degree and average fitness of the sub-population, the topological direction of migration is decided adaptively, avoiding the blindness and

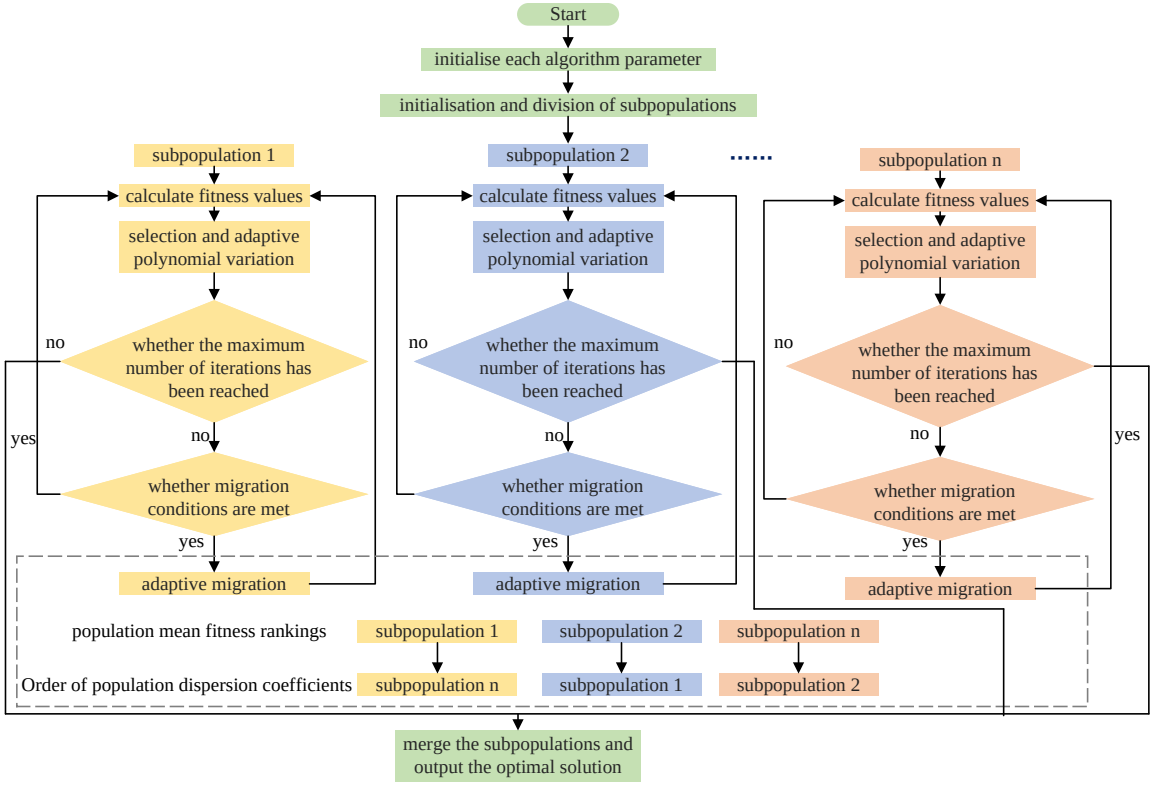

Figure 3. Improvement of the genetic algorithm process

fixity of traditional parallel genetic algorithm migration. The degree of population dispersion is represented by the population dispersion coefficient η in Equation (10), and the average fitness of the population is $f_{\text{avg}} = \sum_{j=1}^{q} f_j/q$, where f_j is a fitness value of the j-th individual of the population and q is the size.

Finally, determine whether the sub-populations satisfy the migration conditions. If each sub-population completes a migration communication operation, otherwise the genetic operation is performed.

4. **Hydroelectric generator excitation control based on improved genetic and RBF neural networks.**

4.1. **Excitation control system RBF network structure establishment.**

Aiming at the characteristics of hydroelectric generator excitation control systems such as large inertia, large hysteresis, and unstable parameters, a hydroelectric generator excitation control mechanism on the ground of an improved genetic and RBF neural network is designed. The radial basis function (RBF) algorithm is chosen to recognize the model. The gradient descent mechanism and the genetic algorithm (GA) are adopted to coarsely and finely adjust the weights of the neural network, respectively. The internal and external perturbations of the system are estimated by the expansion controller, and the nonlinear state error feedback control law is combined with the excitation engine control strategy to deal with the problems of system inertia, hysteresis, and perturbation. The control system structure is implied in Figure 4.

The excitation control system RBF network structure is implied in Figure 5, where the whole structure is divided into an input layer, a fuzzification layer, a fuzzy inference layer, and an output layer. In Figure 5, x_j denotes one water input.

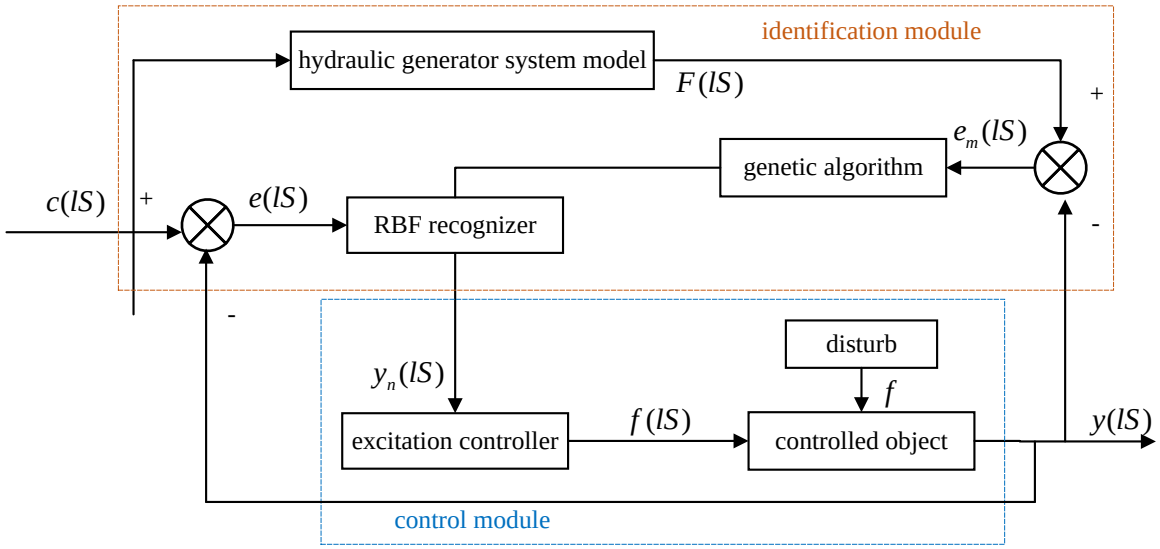

Figure 4. The designed control system structure

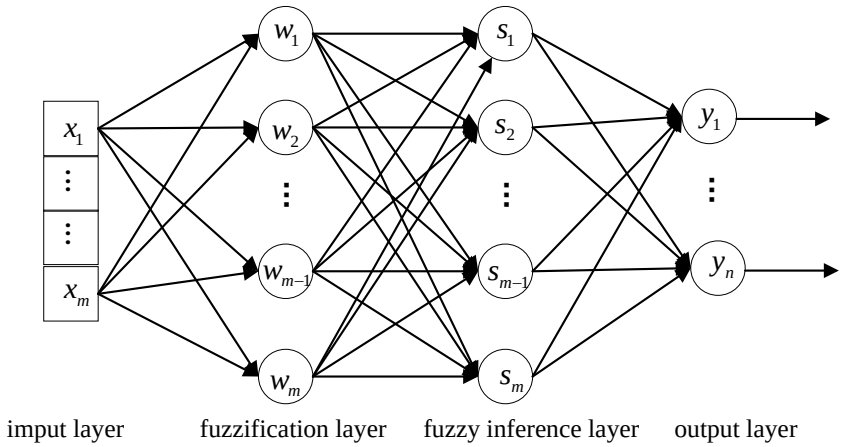

Figure 5. The excitation control system RBF network structure

The original level is the stimulus level, that is assumed to have m nodes, and the nodes are directly jointed in the stimulus components, and the output result for each j layer is: $h_m(j) = x_j$.

The second level is the fuzzification layer; for the nonlinear characteristics of the hydraulic excitation control system, the Gaussian basis function is adopted as the affiliation operation, and the affiliation function formula is as follows.

$$\text{gus}_i = \frac{-(h_1(j) - d_{ij})^2}{(a_i)^2} \tag{19}$$

$$h_2(i,j) = \exp(\text{gus}_i) \tag{20}$$

where d_{ij} denotes the mean value of the affiliation operation of RBF in the j-th fuzzy set of the i-th stimulus t variable; a_i denotes the standard deviation of the affiliation function.

The third layer is the obscured illation level, the obscured illation level has a total of M nodes, and the output of every node is the product of the whole fuzzy sets of the node's inputs: $h_3(i) = \prod_{i=1}^{m} h_2(i,j)$.

The fourth layer is the output layer that realizes the output of the reasoning between the rules: $h_4(m) = Gh_3 = \sum_{i=1}^{M} v(m,i)h_3(i)$.

4.2. **Improving genetic algorithm fine-tuning parameters.** For the purpose of avoiding adopting the genetic algorithm to select too wide a range of parameters, the initial parameters are modified by the gradient descent mechanism, and then the GA improved in the previous section is used to search for the optimization around this set of parameters.

(1) Gradient descent method for coarse tuning of initial parameters. The output layer weights are first adjusted using the following equation.

$$\Delta W(l) = -\mu\frac{\partial E}{\partial w} = -\mu\frac{\partial E}{\partial e_n}\frac{\partial e_n}{\partial g}\frac{\partial y}{\partial w} = \mu e_m(l)h_3 \tag{21}$$

(2) Next, the mean value of the affiliation function is adjusted.

$$\Delta d_{ij}(l) = -\mu\frac{\partial E}{\partial d_{ij}} = -\mu\frac{\partial E}{\partial gus_i}\frac{\partial gus_i}{\partial d_{ij}} = \mu We_m(l)h_3\frac{2(h_1(j) - d_{ij})}{(a_i)^2} \tag{22}$$

(3) The standard deviation of the affiliation function is then adjusted.

$$\Delta a_i(l) = -\mu\frac{\partial E}{\partial a_i} = -\mu\frac{\partial E}{\partial gus_i}\frac{\partial gus_i}{\partial a_i} = -\mu We_m(l)h_3\frac{(h_1(j) - d_{ij})}{(a_i)^3} \tag{23}$$

where μ is the learning rate and its value range is $\mu \in (0,1)$.

At last, genetic algorithms are used to find the optimization.

Step1: Coding and initializing the population. The mean, standard deviation and weights generated by the gradient descent method are divided by uniform distribution for real number coding. Firstly, the main space is divided into T subspaces, secondly, each subspace is quantized and N individuals are selected by using the uniform array, and finally, from the $T \times N$ individuals, the peculiars with the greatest fitness are selected as the initial population. To reduce the error value between the excitation control system model and the actual output, the output fitness function is chosen as the Euclidean distance between the ideal value and the actual value, and the fitness function formula is as follows.

$$C(x,j) = \sqrt{\frac{1}{M}\sum_{S=1}^{m}\left(y_n(lS) - y_n(lS+S)\right)^2} \tag{24}$$

Step2: Remove a definite amount of peculiars from the population each time (put-back sampling) and select the greatest adapted one into the offspring population. Repeat this operation until the novel population size reaches the innovative population size. The new population set is: $Q(j) = C^*(x_j)$.

Step3: After the crossover is completed, the peculiars will be inverted by changing the values of certain loci in the coding of the peculiars in the population with the credibility of mutation. If the novel peculiar has a better fitness value than the original individual, the novel individual will be retained, otherwise the original individual will be retained.

Step4: The optimized mean value d_{ij}^*, standard deviation a_i^* and weights $\hat{w}$ of the final genetic algorithm are substituted back into the Gaussian basis function of the RBF neural network of the excitation control system.

4.3. **Design of hydro generator excitation control strategy.** The hydro generator excitation control system consists of three parts: Tracking Differentiator (TD), Expansion

State Observer (ESO) and Nonlinear State Error Feedback Control Law (NLSEF). The TD equation is as follows:

$$\begin{cases} \dot{x}_1 = x_2 \\ \dot{x}_2 = Sx_2 - D\text{sat}(x_1 - x_2, \theta) \end{cases} \tag{25}$$

where x_1 is the output signal of primary air volume of tracking control system, x_2 is the change rate of the output signal x_1, S is the filtering factor of excitation control model, D is the change factor of control model, sat() is the saturation function to improve the tracking differentiator, and θ is the switching variable of the output signal.

$$\text{sat}(x, \theta) = \begin{cases} \text{sign}(x), & |x| \geq \theta \\ \frac{x}{\theta}, & |x| < \theta \end{cases} \tag{26}$$

By designing the excitation control system expansion state observer for the actual output y of the model, the object containing unknown perturbations within the system is transformed into an integral object, and the equation of the expansion state observer is as follows.

$$\begin{cases} \dot{z}_1 = z_2 - \xi_1 s(\theta_1) \\ \dot{z}_2 = z_3 - \xi_2 s(\theta_1) + Au(t) \\ \dot{z}_3 = -\xi_3 s(\theta_1) \end{cases} \tag{27}$$

where $s(\theta)$ is the disturbance estimate of the excitation controller output, z_1 and z_2 implied the tracking signal and the various component of the tracking signal of the identified excitation control system output y, z_3 is the observed value of the nonlinear function of the excitation control system, and ξ_1, ξ_2, and ξ_3 are the error correction gains.

With the known primary water quantity tracking output signals x_1, x_2 and the output values z_1, z_2 of ESO, the tracking primary water quantity error signal of the construction system is the Equation (28).

$$\begin{cases} e_1 = x_1 - z_1 \\ e_2 = x_1 - z_2 \end{cases} \tag{28}$$

Based on the error provided by Equation (28), the following nonlinear configuration is designed to realize the control component of NLSEF.

$$u = \varepsilon_1 \text{fal}(e_1) + \varepsilon_2 \text{fal}(e_2) \tag{29}$$

where ε_j is the adjustable parameter, $fal(e_j)$ is the control function.

5. Experiment and analysis.

5.1. Excitation control system immunity control simulation.

To verify the effect of the control algorithm in this article on the excitation control system of a hydroelectric generator, MATLAB/SIMULINK software is adopted for simulation. The control parameters of the excitation control system are selected with reference to literature [29], the tracking differentiator model change factor $D = 100$, the expansion state observer correction gain $\xi_1 = 50$, $\xi_2 = 500$, $\xi_3 = 1000$, and the parameter $\vartheta = 0.05$ in the Nonlinear State Error Feedback Sliding Mode Control Law (NLSEFSM). For convenience of description, the literature [30] is denoted as PCPA and the algorithm in this paper is denoted as HGEC.

The parameters of the GA-optimized RBF are a 0.1 learning rate, 0.3 momentum factor, 100 populations, 10 parameters per chromosome, 100 iterations, 0.1 initial crossover rate, 0.1 initial variance rate, and 0.001 target accuracy. A comparison of GA-optimized RBF approximation image and traditional RBF approximation image is shown in Figure 6.

From Figure 6, the mean-square sum of the errors of the GA-optimized RBF designed in this paper is 0.6924, and the mean-square sum of the errors of the traditional RBF is 18.6247. The GA-optimized RBF algorithm has a mean-square sum of errors two orders of magnitude lower than that of the traditional RBF algorithm, and it can approximate the excitation control system model effectively.

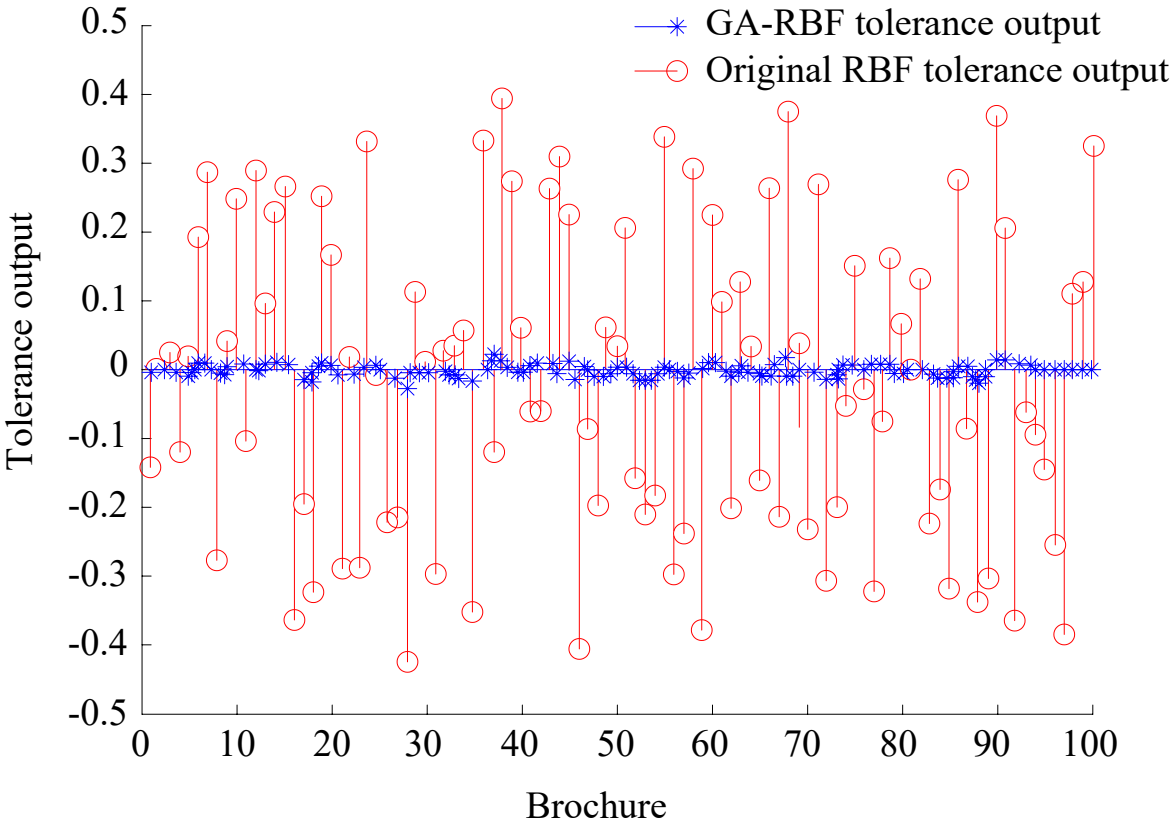

Figure 6. Comparison of Error

To simulate the system, the synchronous generator is made to run under the load condition, and the load is made to produce a step change by changing the model parameters to compare the four control strategies, namely, series PID, sliding mode control, self-immunity control, and HGEC control. Meanwhile, in order to observe the system's ability to resist disturbances, a 10% disturbance is applied when the system is running for 240 s. To verify the superiority of the HGEC algorithm in the face of strong disturbances, the HGEC algorithm is designed to be compared with the similar PCPA control algorithm. Under the condition of unchanged setting parameters, a positive 10% interference is applied to the system at 240 s, and the comparison of control effect is shown in Figure 7.

As shown in Figure 7, when the control system models are the same, the overshoots of PCPA and HGEC are 8.37% and 0% before applying the perturbation, and the regulation times are 56.1 s and 45.3 s. After applying a forward step perturbation with an amplitude of 10% for 240 s, the overshoots of PCPA and HGEC are 13.29% and 4.12%, and the regulation times are 48.3 s and 36.9 s. Comparison shows that HGEC can respond faster to the disturbance than the excitation control with disturbance observer, but both control strategies can respond faster to the disturbance. 36.9 s. Comparison shows that the

HGEC control strategy can respond faster than the excitation control with disturbance observer, but the HGEC control strategy produces less overshoot and the system stability is superior.

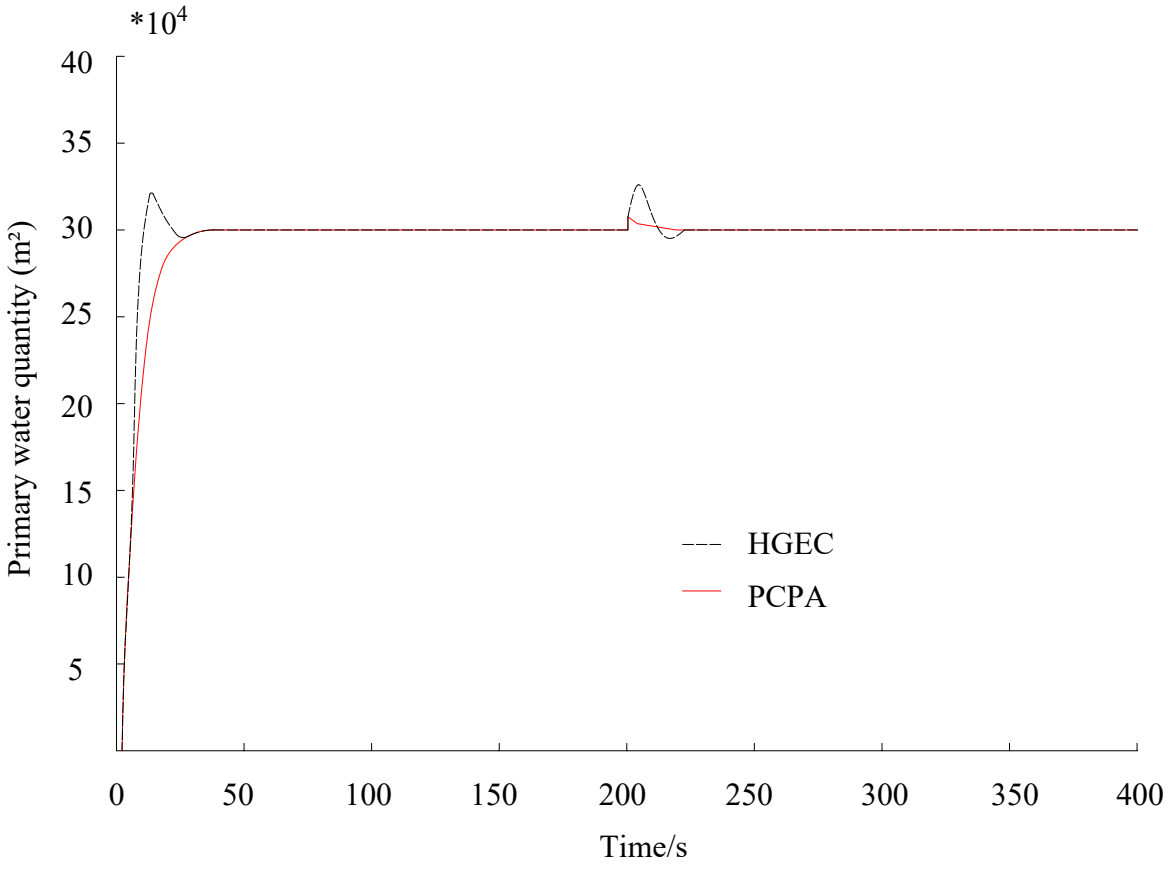

Figure 7. Comparison of control effect

5.2. **Analysis of experimental results.** The results of the experiments were tabulated, and the error between the outputs of the HGEC model and the PCPA model and the output of the original model were calculated and expressed as a percentage. The results were summarized in Table 1.

Table 1. Experimental results and error analysis.

Process	Performance Indications	Original model	HGEC	PCPA
impulse process	output stability value	1	1	1
	overshoot	16.21%	16.94%	19.51%
	adjusting time	13.59s	12.83s	17.63s
	number of oscillations	1	1	1
load step	output stability value	0.8527	0.8591	0.9533
	overshoot	7.63 %	7.14%	9.61%
	adjusting time	11.95s	12.46s	15.93s
	number of oscillations	3	3	4
load shedding	output stability value	0.9381	0.9452	0.9862
	overshoot	23.19%	23.83%	26.74%
	adjusting time	9.72s	9.62s	13.91s
	number of oscillations	2	2	3

By observing the results of the original model with the HGEC model and the PCPA model, it can be found that the amount of oscillations in the dynamic performance of the HGEC model and the original model are the same in the three simulation tests, and the number of oscillations of the PCPA model in the load step and load dumping phase are 4 and 3, respectively, which are different from that of the original model. This is related to the tracking differential regulation performance of the controller, and the optimized HGEC model using genetic algorithm can quickly regulate the generator stator electromotive force to within 5% error when the hydro generator excitation and load change. In contrast, the overshooting error of the PCPA model is larger, which is related to the accuracy of the algorithm. Since the excitation controller is a multi-link nonlinear dynamic link, when the system dynamics changes, the error of the identification results of each link parameter will have an impact on the dynamic performance of the system, especially the overshooting amount, which correspondingly amplifies the output results of the system in the perturbed state, resulting in a larger overshooting amount error between the PCPA model and the original system model. The HGEC model optimizes the parameters and improves the accuracy of the algorithm by improving the genetic algorithm, so that the overshooting error is controlled within 1%, and the absolute value of the error is less than 1%, which is still more accurate in describing the dynamic performance of the system, and it has a certain degree of applicability in evaluating the state of the hydro generator excitation controller. The outcome of this experiment indicates that the HGEC model suggested in this article has good accuracy and usability.

6. **Conclusion.** In this paper, a hydroelectric generator excitation control based on improved genetic and RBF neural networks is proposed to address the problem of unstable parameters of existing excitation control methods. Firstly, the genetic algorithm is optimized to take advantage of the natural parallelizability of GA to separate the initial population into multiple sub-populations, and each sub-population performs the genetic operation concurrently without interfering with each other, which helps to maintain the diversity of the population, avoid falling into the locally optimal solution, and improve the quality of the solution. Then a hydroelectric generator excitation control method based on improved genetic and RBF neural networks is designed, which selects the RBF algorithm to recognize the model, coarsely adjusts and finely adjusts the neural network weights by gradient descent and genetic algorithms, respectively, and estimates the internal and external perturbations of the system by expanding the controller, and combines the nonlinear state-error feedback control law and the excitation engine control strategy in order to overcome system inertia, hysteresis and perturbation. The experimental results indicate that the method suggested in this article has low output stabilization value, overshooting amount, regulation time and vibration number errors, and exhibits good stability performance.

REFERENCES

[1] H. X. Zhang, and L. X. Miao, "Modeling and Experiment on Active Vibration Control of Hydraulic Excitation System," *Applied Mechanics and Materials*, vol. 187, pp. 130-133, 2012.

[2] W. Zhu, Y. Zheng, J. Dai, and J. Zhou, "Design of integrated synergetic controller for the excitation and governing system of hydraulic generator unit," *Engineering Applications of Artificial Intelligence*, vol. 58, pp. 79-87, 2017.

[3] M. Taghizadeh, and M. Javad Yarmohammadi, "Development of a self-tuning PID controller on hydraulically actuated stewart platform stabilizer with base excitation," *International Journal of Control, Automation and Systems*, vol. 16, pp. 2990-2999, 2018.

[4] E. Rebollo, F. R. Blanquez, C. A. Platero, F. Blazquez, and M. Redondo, "Improved high-speed de-excitation system for brushless synchronous machines tested on a 20 MVA hydro-generator," *IET Electric Power Applications*, vol. 9, no. 6, pp. 405-411, 2015.

[5] L. G. Scherer, R. V. Tambara, and R. F. de Camargo, "Voltage and frequency regulation of standalone self-excited induction generator for micro-hydro power generation using discrete-time adaptive control," *IET Renewable Power Generation*, vol. 10, no. 4, pp. 531-540, 2016.

[6] D. Xia, and G. Heydt, "Self-tuning controller for generator excitation control," *IEEE Transactions on Power Apparatus and Systems*, vol. 2, no. 6, pp. 1877-1885, 1983.

[7] J. B. Devotta, "A dynamic model of the synchronous generator excitation control system," *IEEE Transactions on Industrial Electronics*, vol. 6, no. 4, pp. 429-432, 1987.

[8] R. C. Schaefer, and K. Kim, "Excitation control of the synchronous generator," *IEEE Industry Applications Magazine*, vol. 7, no. 2, pp. 37-43, 2001.

[9] M. Galaz, R. Ortega, A. S. Bazanella, and A. M. Stankovic, "An energy-shaping approach to the design of excitation control of synchronous generators," *Automatica*, vol. 39, no. 1, pp. 111-119, 2003.

[10] O. P. Malik, "Amalgamation of adaptive control and AI techniques: applications to generator excitation control," *Annual Reviews in Control*, vol. 28, no. 1, pp. 97-106, 2004.

[11] P. Maya-Ortiz, and G. Espinosa-Pérez, "Output feedback excitation control of synchronous generators," *International Journal of Robust and Nonlinear Control: IFAC-Affiliated Journal*, vol. 14, no. 9-10, pp. 879-890, 2004.

[12] S. Fan, C. Mao, and L. Chen, "Optimal coordinated PET and generator excitation control for power systems," *International Journal of Electrical Power & Energy Systems*, vol. 28, no. 3, pp. 158-165, 2006.

[13] G. Fusco, and M. Russo, "Nonlinear control design for excitation controller and power system stabilizer," *Control Engineering Practice*, vol. 19, no. 3, pp. 243-251, 2011.

[14] A. Saavedra-Montes, J. Ramirez-Scarpetta, C. Ramos-Paja, and O. Malik, "Identification of excitation systems with the generator online," *Electric Power Systems Research*, vol. 87, pp. 1-9, 2012.

[15] P. Zhao, W. Yao, J. Wen, L. Jiang, S. Wang, and S. Cheng, "Improved synergetic excitation control for transient stability enhancement and voltage regulation of power systems," *International Journal of Electrical Power & Energy Systems*, vol. 68, pp. 44-51, 2015.

[16] T. K. Roy, M. A. Mahmud, W. Shen, and A. M. T. Oo, "Nonlinear adaptive excitation controller design for multimachine power systems with unknown stability sensitive parameters," *IEEE Transactions on Control Systems Technology*, vol. 25, no. 6, pp. 2060-2072, 2016.

[17] M.-d. Wang, B. Kong, X.-y. Li, and X.-k. Wang, "Grey prediction theory and extension strategy-based excitation control for generator," *International Journal of Electrical Power & Energy Systems*, vol. 79, pp. 188-195, 2016.

[18] X. Nan, C. Weimin, Q. Dezhi, and L. Lan, "Research of Micro Hydro Power Control Based on Self-excited Induction Generator," *Recent Patents on Computer Science*, vol. 10, no. 4, pp. 340-346, 2017.

[19] H. J. Baesmat, and M. Bodson, "Suppression of sub-synchronous resonances through excitation control of doubly fed induction generators," *IEEE Transactions on Power Systems*, vol. 34, no. 6, pp. 4329-4340, 2019.

[20] T. Orchi, T. K. Roy, M. A. Mahmud, and A. M. Oo, "Feedback linearizing model predictive excitation controller design for multimachine power systems," *IEEE Access*, vol. 6, pp. 2310-2319, 2017.

[21] K. Kawabe, M. Masuda, and T. Nanahara, "Excitation control method based on wide-area measurement system for improvement of transient stability in power systems," *Electric Power Systems Research*, vol. 188, 106568, 2020.

[22] H. Erol, "Delay margin computation of generator excitation control system by using fractional order controller," *Transactions of the Institute of Measurement and Control*, vol. 42, no. 13, pp. 2465-2474, 2020.

[23] P. Jankee, D. T. Oyedokun, and H. K. Chisepo, "Dynamic response of power systems with real GICs: Impact on generator excitation control," *IEEE Transactions on Power Delivery*, vol. 37, no. 6, pp. 4911-4922, 2022.

[24] A. Agarala, S. S. Bhat, and I. Srivastava, "Transient stability analysis of dual excited synchronous generator with excitation control," *Energy Reports*, vol. 9, pp. 242-252, 2023.

[25] K. Wang, Z. Chen, X. Dang, X. Fan, X. Han, C.-M. Chen, W. Ding, S.-M. Yiu, and J. Weng, "Uncovering Hidden Vulnerabilities in Convolutional Neural Networks through Graph-based Adversarial Robustness Evaluation," *Pattern Recognition*, vol. 143, 109745, 2023.

[26] A. L. H. P. Shaik, M. K. Manoharan, A. K. Pani, R. R. Avala, and C.-M. Chen, "Gaussian Mutation–Spider Monkey Optimization (GM-SMO) Model for Remote Sensing Scene Classification," *Remote Sensing*, vol. 14, no. 24, 6279, 2022.

[27] T.-Y. Wu, H. Li, and S.-C. Chu, "CPPE: An Improved Phasmatodea Population Evolution Algorithm with Chaotic Maps," *Mathematics*, vol. 11, no. 9, 1977, 2023.

[28] T.-Y. Wu, A. Shao, and J.-S. Pan, "CTOA: Toward a Chaotic-Based Tumbleweed Optimization Algorithm," *Mathematics*, vol. 11, no. 10, 2339, 2023.

[29] L. Sun, Q. Hua, D. Li, L. Pan, Y. Xue, and K. Y. Lee, "Direct energy balance based active disturbance rejection control for coal-fired power plant," *ISA Transactions*, vol. 70, pp. 486-493, 2017.

[30] J. I. Da Silva Filho, R. A. B. de Oliveira, M. C. Rodrigues, H. M. Côrtes, A. Rocco, M. C. Mario, D. V. Garcia, J. M. Abe, C. R. Torres, and V. B. D. Ricciotti, "Predictive Controller Based on Paraconsistent Annotated Logic for Synchronous Generator Excitation Control," *Energies*, vol. 16, no. 4, pp. 1934, 2023.